

Methods for Droplet Size Distribution Determination of Water-in-oil Emulsions using Low-Field NMR

Nils van der Tuuk OPEDAL¹, Geir SØRLAND², Johan SJÖBLOM¹

¹Ugelstad Laboratory, Department of Chemical Engineering, the Norwegian University of Science and Technology (NTNU), N-7491 Trondheim, Norway.

²Anvendt Teknologi AS

Corresponding author: Nils van der Tuuk Opedal, Dept of Chemical Engineering, the Norwegian University of Science and Technology (NTNU), E-Mail:

nils.opedal@chemeng.ntnu.no

Abstract

A method using Pulsed Field Gradient Nuclear Magnetic Resonance PFG-NMR for water-in-crude oil emulsion droplet size determination has been optimized and compared with optical microscope for validation. The method applies a combination of Pulsed-Field Gradient (PFG) NMR, Stimulated Echo (STE), and Carr-Purcell-Meiboom-Gill (CPMG) sequences for measuring diffusion, resolving oil and water signal and for measuring the attenuation due to a distribution in T_2 values. This returns the droplet size distributions of water-in-oil emulsions within a minute. No prior assumption is made on the shape of the droplet size distribution, which enables the method to resolve for instance bimodal distributions. To validate this method, three different crude oils were used in the experiment. The emulsions prepared had water cuts from 10 to 40 %. The correlation between PFG-NMR and optical microscopy was good for the emulsions. Any potential discrepancies between the two techniques are discussed, so are the limitations and advantages of the methods.

Keywords:

Water-in-oil Emulsions, Droplet Size Distribution, PFG, NMR, Diffusion.

1 Introduction

The behavior of emulsions is of great importance for a variety of industries and sciences. Independent of the origin of the emulsion, whether it be the mostly unwanted emulsions relevant for the petroleum industry, or emulsions within daily life products such as food and pharmaceuticals. Either way, the mechanisms of emulsion formation and stability are more or less similar for all industries. So, in order to fully appreciate the behavior of an emulsion, a complete characterization is purposeful. One of the important features of an emulsion is its Droplet Size Distribution (DSD). The droplet size influences many characteristics, for instance the rheology [1] [2], and the stability of an emulsion [3] and emulsion liquid membrane performance [4]. There are presently several different techniques available to obtain the DSD. The suitability of the techniques, the quality and reliability of the measurements, and the ease at which to use them depends on the system to be studied. Some of the techniques require some kind of preparation which may alter the state of the sample. Other techniques consider only a small portion of the sample, making the results less representative. For instance, the use of light scattering to obtain the DSD for a petroleum emulsions is not ideal due to the impermeability of light through the sample. Thus, if any droplets are measured at all, only the droplets in vicinity of the container wall are included in the measurement. This technique is also not ideal for concentrated emulsions. In addition, light scattering does not discriminate between single droplets and clusters. [5] The microscope is another popular technique. This technique often requires dilution, and in addition to being potentially tedious and labour intensive, there are wall effects to consider when the emulsion drop is flattened between two glass slides, and only a small part of the sample is analyzed. [6] The advantages by using NMR to obtain the DSD are several. The entire sample is considered, no sample preparation or dilution is required and the measurements can be relatively fast. The non-perturbing handling of the sample means that the same sample can be analyzed several times. For characterization of water-in-crude oil emulsions, the technique is especially useful due to the opacity of petroleum crude oils.

Stejskal and Tanner [7, 8] pioneered the work on restricted diffusion by studying the diffusion using the pulsed field gradients (PFG-NMR) experiment, where they utilized the difference in the relaxation times for oil and water to separate the signals. Since this initial work on restricted diffusion, the method has been further developed to its current status where it

amongst a broad range of applications may be used to characterize various food emulsions [9, 10] [11] [12] and crude oil emulsions [13]. As the NMR experiment can be performed in numerous ways, a large variety of approaches have been developed for this purpose. Even though the size determination using different NMR approaches has been compared with other techniques with promising results, many of the methods are based on the work by Packer and Rees [14] with the assumption that the shape of the distribution follows a log-normal distribution [15] [12] [16] [17] [9] [18]. Most droplet size distributions do follow a log-normal distribution. However, it might not be the case for all systems. The loss of accuracy in the determined distribution shape can be of importance in order to fully understand the behavior of an emulsion.

Peña and Hirasaki [19] included a CPMG sequence to avoid the a priori assumption of a well defined shape of the distribution. But they still applied the same diffusion model as used by Packer and Rees to find the droplet sizes. One should also bear in mind that these methods assumes a mono exponential decay of the oil signal due to longitudinal relaxation. This is not the case in for example crude oil emulsion, where the relaxation components from the crude oil may vary several orders of order of magnitude.

Aichele et al [13] presented a technique using PFG-NMR with diffusion editing (DE) to quantify brine/crude oil emulsions. This technique made no assumptions on the distribution shape. However, each measurement was relatively long, 5 -7 hours, and proved sensitive to coalescence.

This work presents a new method which uses a combination of Pulsed Field Gradient (PFG), Stimulated Echo (STE) and CPMG sequences to obtain the DSD for crude oil emulsions within a minute. The method combines either the short diffusion time model developed by Mitra et al [20] or a slight modification of the method presented by Packer and Rees [14] with a method for determination of pore size distributions in brine saturated rock core plugs developed by Sørland et.al [21]. The major difference from brine saturated rock core plugs is that the continuous phase, being either oil or water, returns an NMR signal that may overlap in the T_2 distributions. Thus we have included a so called z-storage interval for resolving oil and water due to non overlap in the T_1 distributions instead. As will be shown in the theoretical section this combined sequence can be used to find the short time diffusion coefficient, the average surface to volume ratio (yielding the average droplet size), the surface relaxivity and the droplet size distribution. The methods make no assumptions on the shape of the distributions, enabling it to resolve less trivial distributions. In order to test the performance of the methods, emulsions of three different crude oils at different water cuts

(volume % of water) were investigated. As a comparison, the droplet sizes of the same emulsions were studied with optical microscope.

2 Theory

2.1 Extracting droplet size distribution from water in oil or oil in water emulsions

Here we recapture the theory leading the functionality between the diffusion coefficient at short observation times and the surface to volume ratio. It is also shown how this can be related to a droplet size distribution. A simple way to combine the asymptotical approach [14] at long observation times with the T_2 distribution from the CPMG experiment to result in droplet size distribution is given in section 2.1.3.

The equation of motion for the diffusing molecules within the cavities may be described by the standard diffusion equation:

$$\frac{\partial G}{\partial t} = D_0 \nabla^2 G \quad (2.1)$$

where the diffusion propagator $G = G(\mathbf{r}_0, \mathbf{r}, t)$, is the conditional probability [22], defined as

$$G = p(\mathbf{r}_0, 0) \times P(\mathbf{r}_0, \mathbf{r}, t) \quad (2.2)$$

where $p(\mathbf{r}_0, 0)$ is the probability of finding the molecule at position \mathbf{r}_0 at time $t = 0$, and $P(\mathbf{r}_0, \mathbf{r}, t)$ is the probability of finding this molecule at position \mathbf{r} at a later time t .

When including the effect from relaxation at the pore walls, the boundary condition can be stated as

$$D_0 \mathbf{n} \cdot \nabla G_{r \in S} + \rho G_{r \in S} = 0 \quad (2.3)$$

Here \mathbf{n} is the outward normal vector on the pore surface S and ρ is the surface relaxivity. The boundary condition merely states that the surface may act as a sink for the coherence of the NMR signal of the molecules, while in the physical picture the molecules collide with the surface and bounce back into the cavity. As seen by the NMR experiment, the molecule, if it relaxes at the surface, vanishes from the heterogeneous system. This is why it is difficult to relate the NMR diffusion experiments to physical properties as described by the diffusion

equation (eq. 2.1) without the surface relaxation term in the boundary condition (eq. 2.3). The existence of a surface relaxation term makes the true physical picture of particles different from the picture of the nuclear magnetic moments of the molecules. Compared to brine saturated rock core plugs, we have found the surface relaxivity, as experienced by the brine, to be approximately two orders of magnitude smaller in emulsion systems ($\rho_{\text{emulsion}} \leq 10^{-6}$ m/s while $\rho_{\text{rock}} \geq 10^{-4}$ m/s). In the following we will focus on two regimes of the ratio between the mean squared displacement and the typical droplet sizes; the asymptotic level of the diffusion coefficient where $(6 D_0 t)^{1/2} \gg R_{\text{cavity}}$ and the short observation time expansion of the diffusion coefficient where $(6 D_0 t)^{1/2} \ll R_{\text{cavity}}$. What is important for these two regimes is the absence of dependency on the surface relaxivity within the equation governing the PFG-NMR experiments. As will be shown in the next sections it is then possible to solve out the surface relaxivity, and thus transform the T_2 relaxation time distributions to droplet size distributions.

2.1.1 The short observation time expansion of the diffusion coefficient

As shown by Mitra et al [20], there is a situation where the surface relaxation term is absent in the solution of the diffusion propagator, i.e. the short time expansion. By assuming piecewise smooth and flat surfaces and that only a small fraction of the particles are sensing the restricting geometries, the restricted diffusion coefficient can be written as

$$\frac{D(t)}{D_0} \approx 1 - \frac{4}{9\sqrt{\pi}} \sqrt{D_0 t} \frac{S}{V} + \varphi(\rho, R, t) \quad (2.4)$$

where $D(t)$ is the time dependent diffusion coefficient, D_0 is the unrestricted diffusion coefficient, in bulk fluid, and t is the observation time. The higher order terms in t , $\varphi(\rho, R, t)$ holds the deviation due to finite surface relaxivity and curvature (R) of the surfaces. At the shortest observation times these terms may be neglected such that the deviation from bulk diffusion depends on the surface to volume ratio alone.

In a porous system a large span in pore sizes must be assumed. eq. (2.4) must be expected to be valid also for a heterogeneous system. If ξ_i is the volume fraction of the pores with surface to volume ratio $(S/V)_i$, eq. (2.4) can be expressed as

$$\sum_i \xi_i \frac{D_i}{D_0} \approx \sum_i \xi_i \left[1 - \frac{4}{9\sqrt{\pi}} \sqrt{D_0 t} \left(\frac{S}{V} \right)_i \right] = \left(1 - \frac{4}{9\sqrt{\pi}} \sqrt{D_0 t} \overline{\left(\frac{S}{V} \right)} \right) \quad (2.5)$$

Measurements of the early departure from bulk diffusion combined with a linear fit of the experimental data to the square root of time will thus result in a value for the average surface to volume ratio $\overline{(S/V)}$.

2.1.2 Transforming a T_2 distribution to a droplet size distribution

Assuming that the water molecules are probing the droplets within the sample, there is a simple relation [23] between T_2 values and the droplet sizes

$$T_2 \approx \frac{V}{S\rho} \quad (2.6)$$

This couples the surface to volume ratio to the surface relaxivity, ρ , and makes it difficult to assign the T_2 distribution to a (V/S) distribution. However, if we make the assumption that eq. (2.6) holds for any droplet size, with ξ_i being the volume fraction of pores with surface to volume ratio $(S/V)_i$ and corresponding relaxation time T_{2i} , we may follow Uh and Watson [24] and write

$$\sum_{i=1}^n \xi_i \frac{1}{T_{2i}} = \sum_{i=1}^n \xi_i \rho_i \left(\frac{S}{V} \right)_i \approx \rho \sum_{i=1}^n \xi_i \left(\frac{S}{V} \right)_i = \rho \overline{\left(\frac{S}{V} \right)} \quad (2.7)$$

Here we have made the basic assumption that the surface relaxivity ρ is independent of droplet size. The left hand side of eq. (2.7) is the harmonic mean $\overline{1/T_2}$ of the T_2 -distribution weighted by the fraction ξ_i of nuclei with relaxation time T_{2i} and n is the number of subdivisions of droplet sizes. This average can be calculated from the T_2 -distribution obtained in a CPMG measurement where the magnetization attenuation $M^{obs}(t)$ is converted to a T_2 distribution by solving an inverse problem using e.g. an Inverse Laplace Transform (ILT) routine [25]. Then the surface relaxivity ρ can be calculated from eq. (2.7) if the average surface to volume ratio $\overline{(S/V)}$ is already found from the diffusion experiment. Finally, the measured T_2 -distribution can be transformed into an absolute droplet size distribution (V/S) by means of the relationship inherent in eq. (2.7).

To sum up, the procedure for deriving absolute droplet size distributions is as follows:

- 1) The average surface to volume ratio $\overline{(S/V)}$ is found from fitting eq. (2.5) to a set of diffusion measurements at short observation times.
- 2) The average (S/V) can be correlated to the average $(1/T_2)$ found from a CPMG experiment. From eq. (2.7) eq. (2.6) can then be written as

$$\left(\frac{1}{T_2}\right) \approx \rho \left(\frac{S}{V}\right) \quad \Rightarrow \quad \rho = \left(\frac{1}{T_2}\right) \times \left(\frac{S}{V}\right)^{-1} \quad (2.8)$$

hence we find the relaxivity, ρ , which then is assumed to be droplet size independent.

- 3) Under the assumption of droplet size independency of the relaxivity the value of ρ can then be used in eq (2.6) thus resulting in a linear relation between T_2 and the volume to surface ratio which is a measure of the droplet size. By multiplying the T_2 distribution by the calculated surface relaxivity the distribution is normalized to a droplet size distribution in absolute length units.

2.1.3 The asymptotic level of the measured diffusivity

As shown by Packer et.al [14], there is a situation where the surface relaxation term is absent in the solution of the diffusion propagator, i.e. for diffusion within closed cavities and when the diffusing molecules have covered mean free path lengths \gg cavity dimension $[(6 D_0 t)^{1/2} \gg R_{\text{cavity}}]$. In such a situation the attenuation of the NMR signal from diffusion within the closed droplet can be simplified to [14] [26]

$$\left(\frac{I}{I_0}\right) \approx \exp^{-\frac{1}{5} \gamma^2 \delta^2 G^2 R^2} \quad (2.9)$$

where δ is the gradient pulse length, G is the applied gradient strength and R is the droplet radius. In a heterogeneous system a large span in droplet sizes must be assumed. Thus eq. (2.9) must be expected to be valid also for a heterogeneous system. If ξ_i is the volume fraction of the droplets with surface to volume ratio $(S/V)_i$, eq. (2.9) can be expressed as

$$\left(\frac{I}{I_0}\right) \approx \sum_i \xi_i \exp^{-\frac{1}{5}\gamma^2\delta^2G^2R_i^2} \quad (2.10)$$

When the exponent in Equation 2.10 is small for all i , we may expand the exponential functions using its two first terms:

$$\left(\frac{I}{I_0}\right) \approx \left(\sum_i \xi_i - \sum_i \xi_i \frac{1}{5}\gamma^2\delta^2G^2R_i^2\right) = 1 - \frac{1}{5}\gamma^2\delta^2G^2\bar{R}^2 \quad (2.11)$$

Where \bar{R}^2 yields the average value of the square of the droplet radius. Measurements of the early departure from I_0 as a function of applied gradient strength may then result in a value for the average surface to volume ratio. This can be used in combination with a T_2 distribution to result in a droplet size distribution as shown in section 2.1.2. The only difference is that the value of the surface relaxivity now must be given as

$$\rho = \sqrt{\left(\frac{1}{T_2^2}\right) \times \left(\frac{\bar{R}^2}{9}\right)} \quad (2.12)$$

2.2 Separation of crude oil and brine signal

There are several ways to separate the NMR contribution of the crude oil and brine components. One method is to suppress the brine using the oneshot method [27]. This applies when the molecular mobility of the oil is more than a decade slower than the mobility of the brine. Another method applies when the T_1 distributions of brine is longer than the T_1 distribution of the crude oil. Then one may store the NMR signal for full recovery of the crude oil signal back to thermal equilibrium while the brine signal still can be measured on. If one of the two methods can be used, the theory above can be applied in achieving a droplet size distribution for the brine droplets. In the following we will focus on the method using z-

storage delay for suppression of the crude oil signal using the sequence shown in figure 3.1. Then we find the following T_2 distributions for short and long z-storage (Δ) intervals, as shown in figure 2.1. By increasing the duration of the z-storage one can thus omit the oil signal. The two peaks at short Δ corresponds to the oil signal (left peak) and water signal(right peak).

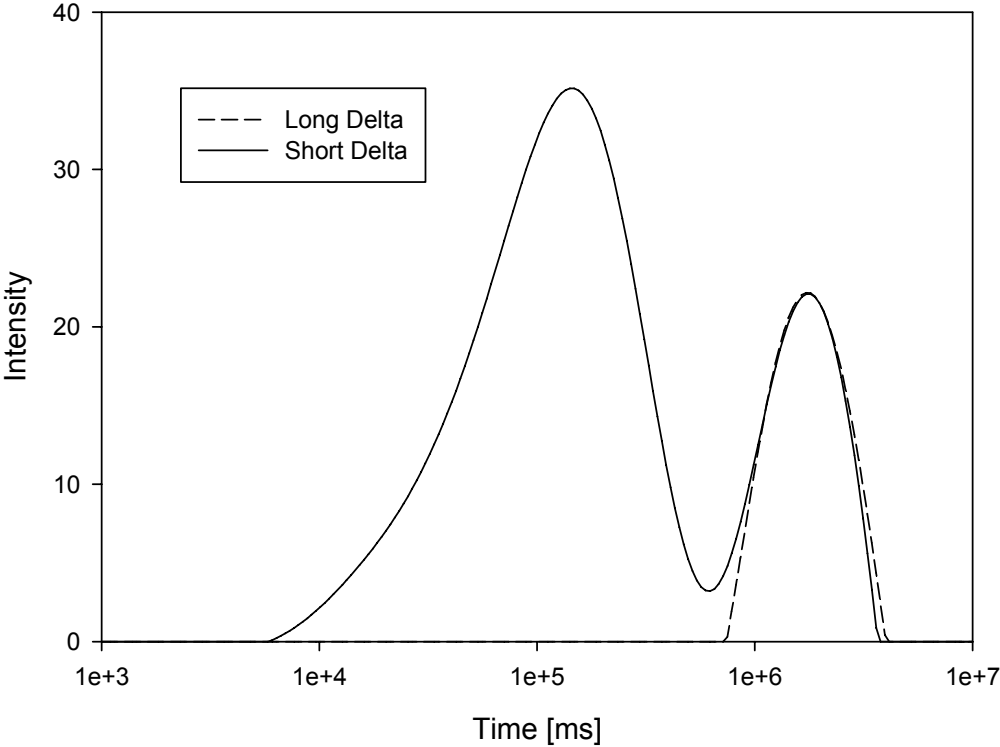


Figure 2.1 The effect of using z-storage to obtain the T_2 distribution of water alone.

3 Experimental

3.1 Materials

Three different petroleum crude oils were used; some of the key properties of the crude oils are given in table 3.1. The crude oils will henceforth be denoted as A, B and C. The water was Milli-Q grade (18,2 m Ω).

Table 3.1 Summary of key crude oil properties at 25 °C.

Crude oil	Density [g/cm ³]	Viscosity [mPas]
A	0.905	53
B	0.932	220
C	0.970	2500

3.2 Methods

3.2.1 Emulsion preparation

The emulsions were prepared by mixing the crude oils with water at room temperature (25°C). The total sample volume of all the emulsions was 15 mL. Water cuts higher than 40% were not investigated as these emulsions were not stable for crude A and B, and since it proved difficult to properly mix the viscous crude C and water at higher water cuts at room temperature. The mixing was performed by an IKA Ultra Turrax homogenizer (10 mm head) with a stirring speed of 24 000 rpm for 2 minutes. The emulsions were analyzed immediately after mixing. Parallel to the NMR measurements, the same emulsions were analyzed with the microscope.

3.2.2 Droplet Size Distribution from Microscope

The microscope consist of a Nikon Eclipse ME 600L Microscope and a CoolSNAP-Pro cf camera with Image-Pro PLUS 5.0 software of Media Cybernetics. By utilizing a costum-made macro that identifies and measures the size and shape of dark objects in a picture, the distribution of the droplets was obtained. The shape measurement was useful to exclude droplets with a non-spherical shape and clusters of droplets. In order to obtain a droplet size distribution by using the microscope technique, the emulsions had to be diluted. The original emulsions were too concentrated for the macro to properly separate and distinguish the

droplets. The dilution was performed by adding $\sim 0,2$ g emulsion drop wise to ~ 2 g of the crude oil, and thereby gently mixing. The droplet size distribution was obtained by placing a small drop of the diluted emulsion on a glass slide. The drop was then flattened by placing a smaller glass slide on top of the droplet. Thereafter, several pictures of the emulsion drop were taken. In order to get a credible impression of the droplet sizes for each emulsion, more than 800 droplets were counted in the distribution population. However, this method proved insufficient for crude C emulsions. Visual observation of the droplets from emulsions prepared with this particular oil was difficult due to its dark appearance and high viscosity. In order to observe the droplets formed from crude oil C, a technique that has been performed previously on heavy viscosity crude oils was used [28]. By placing a small drop of the emulsion on the glass slide, and then placing a small drop of toluene in contact with the emulsion drop, the water droplets diffuse into the toluene phase/drop. The droplets diffused into the toluene zone were then registered and measured in the same manner as the other two crude oils.

3.2.3 Droplet Size Distribution from NMR

The NMR sequences that were used for measuring the droplet size distributions of the oil/water systems are explained in the following section. The NMR measurements were performed on a low field Oxford Instruments MARAN Ultra spectrometer, 23 MHz tempered at 40°C , with the ability of producing shaped gradients up to 400 G/cm. The NMR sample tubes of 18 mm diameter were filled with ~ 3 mL of the emulsion.

The PFG-NMR as shown in figure 3.1 makes use a combination of three different sequences to obtain the DSD. The first part is the 11-interval PFG sequence used to weight the NMR signal with a diffusion dependent term. Originally this sequence was developed for diffusion studies in the presence of internal magnetic field gradients. In an emulsion system we find the internal gradient strengths to be negligible, but still we are using the 11-interval PFG sequence in order to minimize the effect from eddy current transients. Thus we may use eddy current dead times of just 500 μs without any sophisticated preemphasis adjustment. In the second part the signal is stored along the z-direction for a period of Δ , which is used for letting the oil signal relax towards thermal equilibrium. Then we are left with water signal only that is subjected to a CPMG sequence [29] in the last part of the sequence. This part may then return a T_2 distribution from water/brine only. This distribution is diffusion weighted depending on the strength on the applied magnetic field gradient g used in the first part of the sequence. When setting the applied gradient strength to zero and Δ long enough to suppress

the crude oil signal, the T_2 distribution obtained can be used to calculate the droplet size distribution. This will then obtain the volume weighted droplet size distribution of the dispersed droplets. An important feature about the CPMG sequence is that it does not make any assumptions on the distribution shape.

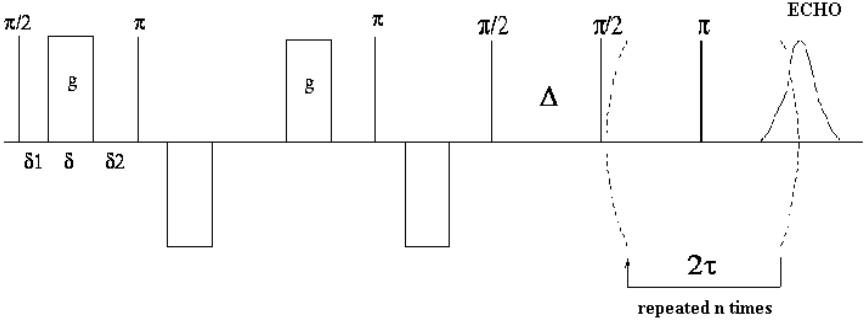


Figure 3.1 Combined Pulsed Field Gradient - Stimulated Echo – CPMG sequence.

3.2.4 The Diffusion- T_1 -weighted profile experiment

In the PFG-NMR sequence shown in figure 3.2 we have replaced the CPMG part with spin echo acquisition during a read gradient. This yields a position dependent NMR signal once it has been Fourier transformed, i.e. a distribution of signal intensities that depends on position within the sample. The gradients in the first part of the sequence may be used to suppress signal from the water, leaving us with the profile of the crude oil component. This may act as a probe of emulsion stability, as a variation of the crude oil profile indicates instability of the emulsion.

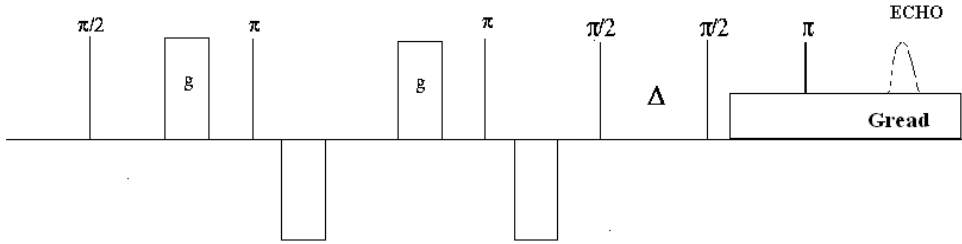


Figure 3.2 The Diffusion- T_1 -weighted profile sequence.

One may also use set the gradients in the first part to zero, and instead make use of the z-storage delay Δ either to measure the profile of the entire sample (short Δ), or the water profile of the sample (long Δ). This is shown in figure 3.3, where the dashed line (long Δ)

indicates that water is moving to the bottom of the sample. The solid lines (short Δ) giving the signal of all components present in the sample tubes indicates a flat intensity profile.

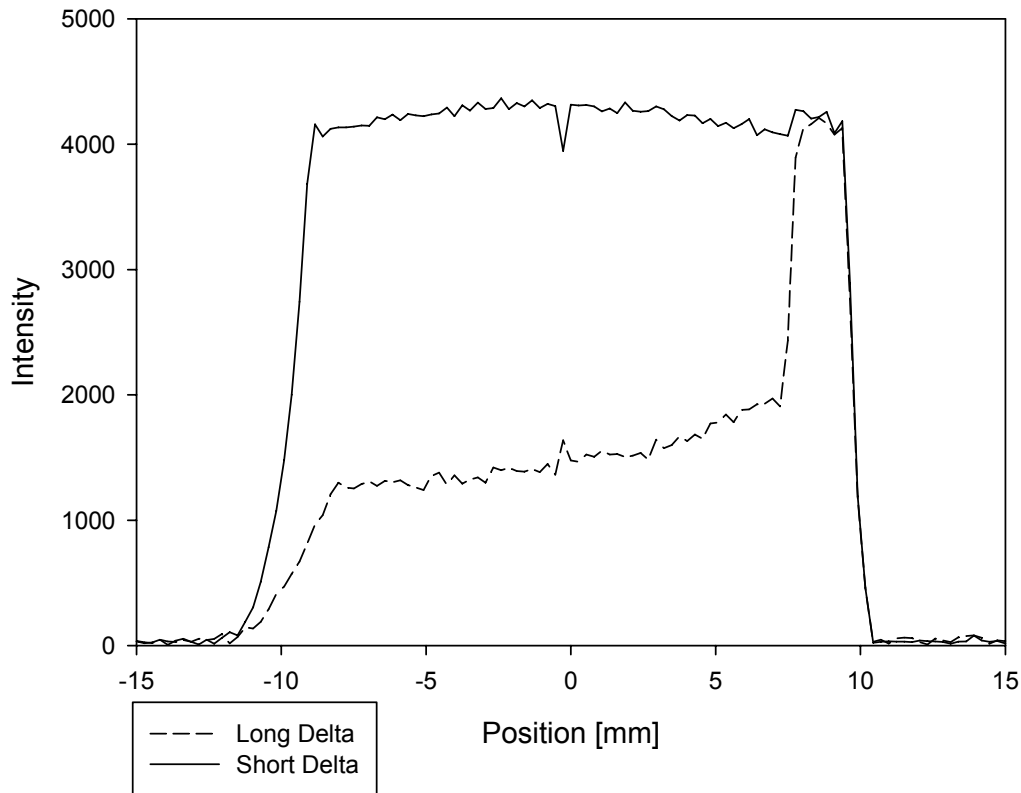


Figure 3.3 The effect of using z-storage to obtain the water profile of the sample. The bottom of the sample is at ~ 10 mm, and the top of the sample is at ~ -10 mm.

As the NMR magnet is tempered to 40°C , and the emulsions were prepared at room temperature, the NMR tubes containing sample had to be tempered for about 15 minutes to reach the magnet temperature. The emulsions were then subjected to the NMR measurements. Depending on the T_2 values of the crude oil, the water signal was separated from the crude oil signal by setting the Δ to 1.5 seconds \pm 0.5 seconds, depending on the T_2 distribution of the crude oil being investigated. In order to study any instability of the emulsions, the NMR experiments were repeated after certain time intervals. The diffusion measurements were calibrated with Milli-Q grade water, and the value of the unrestricted diffusion coefficient, D_0 , was measured to be $3.2 \times 10^{-9} \text{ m}^2/\text{s}$.

4 Results & Discussion

The outline of the experimental data obtained will here be presented. However, the manner in which the results from the two techniques will be presented requires a short comment. A distribution obtained from image analysis of droplets in a microscope will give a size distribution based on number intensity. The NMR method yields a volume-based size distribution; the droplet dimensions are calculated from the surface to volume ratio. This means that a direct comparison of the results from the two techniques might not give the best correlation. A number based size distribution will yield a smaller mode and be differently shaped compared to a volume based size distribution. Figure 4.1 illustrates the difference of weighting by a number- and volume-based distribution obtained by the NMR. In a volume-based distribution, the smallest droplets will be discriminated by the larger ones, and vice versa. In the section where the two techniques are compared, the volume based distribution obtained from the NMR has been changed/transformed to a number based distribution by dividing the volume intensity of each diameter interval by its volume. The opposite could have been done; transforming the number-based distribution of the microscope to a volume-based one. However, due to the low amount of data points compared to the NMR data, such a transformation could easily become flawed. If a certain data set would contain one or two droplet relatively larger than the other ones, the transformed distribution would be skewed by these particular droplets. The distributions presented from both techniques are also normalized.

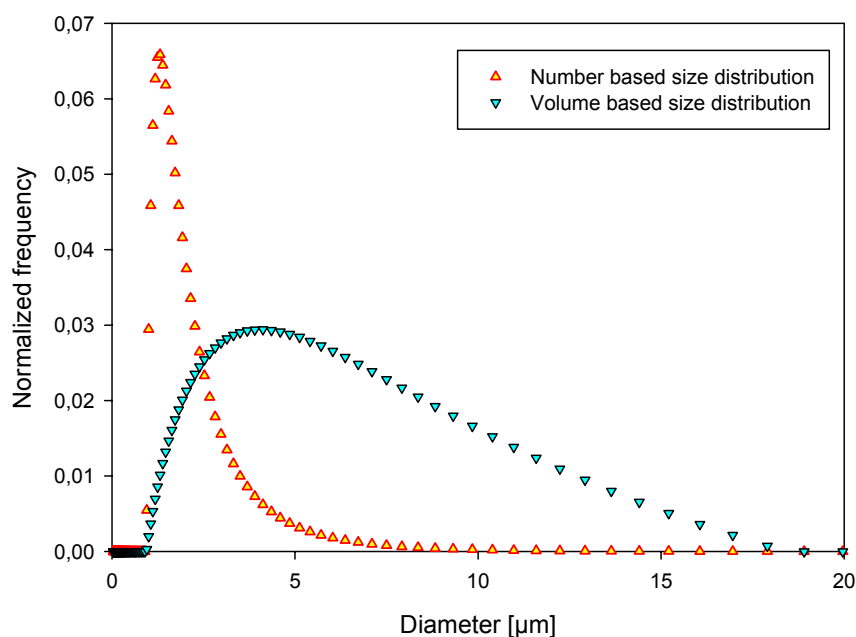


Figure 4.1 Volume-based and number-based size distribution of crude A emulsion with 10 % water cut obtained by NMR.

4.1 Separation of oil and water signal in the NMR

The NMR technique herein presented utilizes the fact that the relaxation times of the ^1H spin are dependent on the molecular structure. And so, separating the signal from oil and water phases is dependent on the nature of the particular phases. The structure of a water molecule is not changeable, but the average molecule size and structure of hydrocarbons found in crude oils may vary. As seen in figure 4.2, the ease at which to distinguish the water and oil signal increases with the viscosity. The signal from the droplets of the emulsion from crude A partially overlaps with the oil signal, making it less trivial to separate the two contributions. Thus, depending on the delay time at which the signal recording starts (Δ , see figure 2.1), either signal from the smallest water droplets might be excluded or signal from the oil might be included. However, there is a clear cut-off between the contribution of water and oil signal in the T_2 distribution for crude B and C.

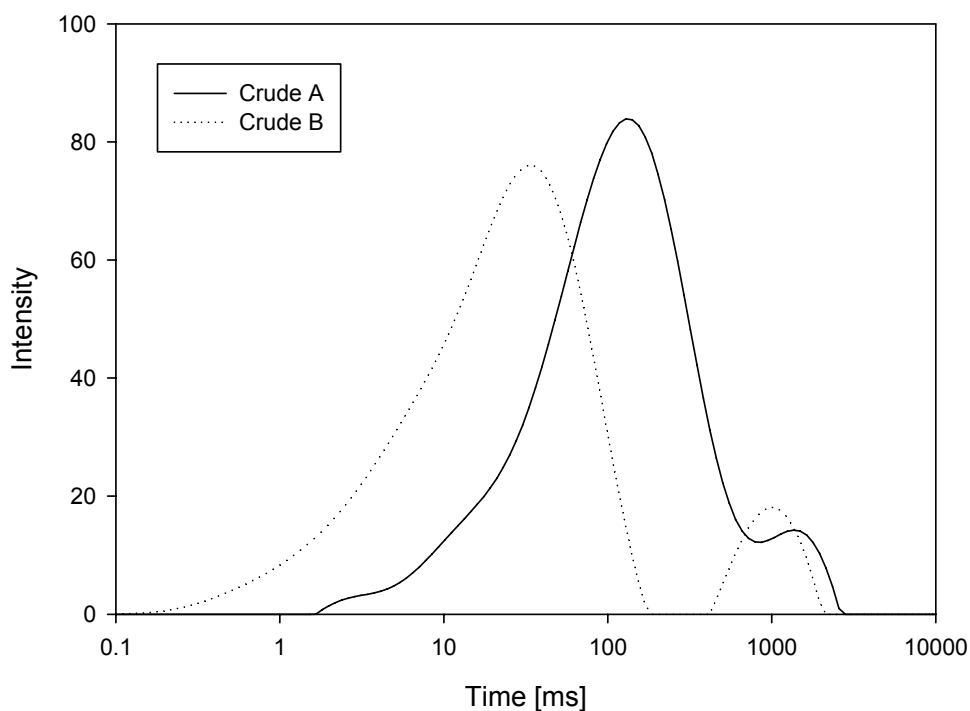


Figure 4.2 T_2 distributions of emulsions with 10 % water cut formed from Crude A and B.

4.2 Accuracy of the Microscope

The microscope technique has its advantage that it gives a direct view of the droplets. A study regarding the accuracy of the microscope technique for obtaining size distributions was performed by Denkova et al [30]. The experimental error of the technique itself proved to be minor. The largest contribution to the error was attributed to the resolution limit of the microscope used. As can be seen from figure 4.3, analyzing an emulsion with different magnification might yield different results. The inclusion of the smallest droplets is dependent on the microscope resolution. Another issue regarding the microscope technique is the dilution of the emulsion. Diluting the continuous phase can be a major intrusion for some systems. For instance, the dilution of margarine can induce coalescence due to the breakdown of crystal networks within these emulsions [16], other emulsions might exhibit increased stability due to addition of more surfactant. Crude oils are known to contain several surfactants. [31] The effect of the dilution on the systems studied herein has not been further explored. Though, diluting could stop droplet collision and coalescence. Another factor is the possible change in solubility properties of interfacial active compounds. This means that even though the same emulsions were studied parallel in the NMR and the microscope, the dilution might result in a different behavior.

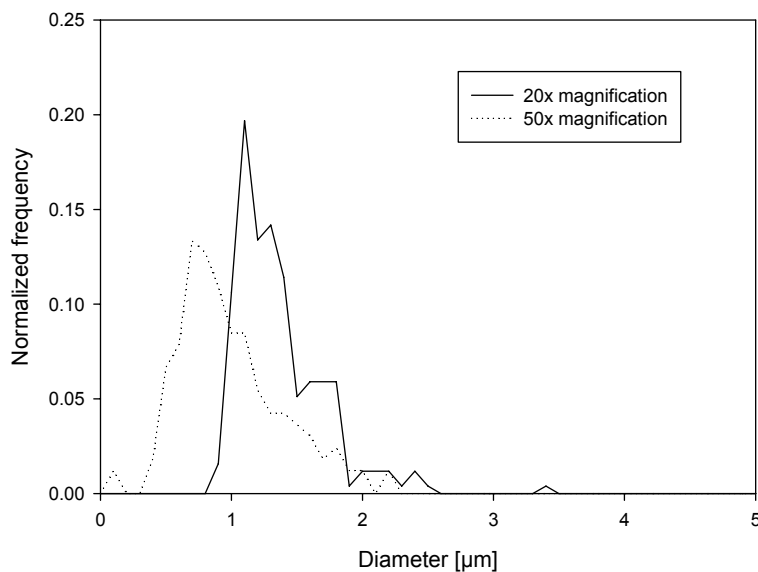


Figure 4.3 Droplet size distribution of an emulsion studied with microscope with different magnification.

4.3 Comparison of the two techniques

Even though the NMR model presented in this paper makes no assumptions of the shape of the distributions, the results indicate that the log-normal fitting is suitable for the number based distributions. Most unimodal emulsion droplet size distributions follow the log-normal distribution [32] [33] [9]. The distribution obtained from the microscope were also fitted with the log-normal distribution. The result of the fitting is given in table 4.1. The log-normal equation is given below:

$$f(a) = \frac{1}{\sqrt{2\pi}\sigma 2a} e^{-\left[\frac{(\ln(2a)-\mu)^2}{2\sigma^2}\right]} \quad (4.1)$$

where a is the droplet radius and σ is the width of the log-normal distribution.

The comparison of the DSD from an emulsion with 10 % water cut for crude A is given in figure 4.4 below. The two distributions correlate well, the distribution peak and the distribution shape are similar for both techniques. As seen from table 4.1 below, the difference of both the mean diameter and standard deviation is minimal. There is a difference between the two graphs for the smallest droplets. The NMR method indicates a distribution with droplets ranging from about 1 μm , whereas the microscope indicates that the smallest droplets are about 0.5 μm in diameter. The difference can be explained due to the T_2

distribution and the selected delay time at which the NMR recording starts; figure 4.2. As mentioned above, an overlapping T_2 distribution means that the signals from the two phases coincide. With that, there is a risk that the contribution from the smallest droplets will not be properly registered with the selected Δ .

Table 4.1 Summary of the log-normal fitting for emulsions of crude A and B.

Crude Oil	Water cut	Parallel	Method	d_0 [μm]	σ
A	10 %	1	Microscope	1,34	0,26
			NMR	1,67	0,30
		2	Microscope	1,42	0,30
			NMR	1,49	0,32
	20 %	1	Microscope	1,43	0,27
			NMR	2,31	0,28
		2	Microscope	1,40	0,34
			NMR	2,83	0,30
B	10 %	1	Microscope	1,34	0,25
			NMR	1,20	0,31
		2	Microscope	1,31	0,29
			NMR	1,01	0,37
	20 %	1	Microscope	1,46	0,20
			NMR	1,84	0,34
		2	Microscope	1,47	0,24
			NMR	1,70	0,36

Figure 4.5 displays the size distribution for an emulsion from crude B. The correlation between the NMR and the microscope is good. The shapes of the two distributions are comparable, and the registered dimensions of the smallest and largest droplets present in the emulsion are similar for both techniques. The fact that the quantification of the smallest droplets tallies for both techniques for crude B, and not for crude A, can be understood by figure 4.2. There is a distinct gap between the T_2 time for the oil and water phases for emulsions of crude B, making it is easier to set Δ for the recording of the water signal without excluding any of the water signal. Hence, there is a higher probability that the contribution

from the smallest droplets will be included. The peak of the distribution between the two techniques does not correlate equally well as to what was the case for crude A. The NMR indicates a distribution peak around 1 μm . However, the accuracy of droplet detection for the microscope decreases with droplet diameters smaller than 1 μm . It is possible to visually detect the smallest droplets, but it is increasingly difficult to properly detect the droplets by the automatic counting macro due to low contrast. This can be a plausible explanation as to why the peak of the distribution from the microscope is slightly larger than the one of the NMR.

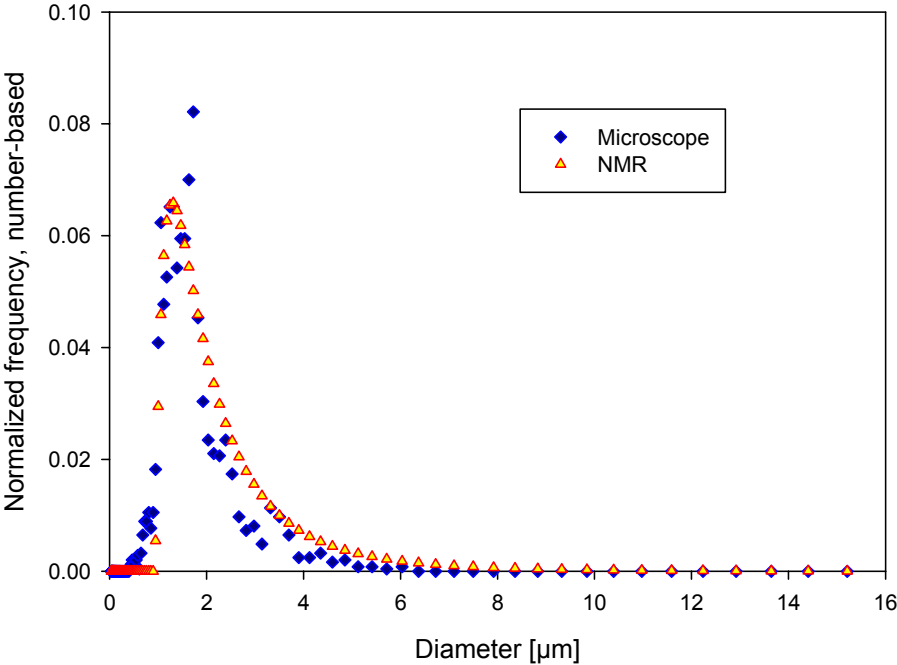


Figure 4.4 Comparison of the DSD of crude A from NMR and microscope; 10% water cut.

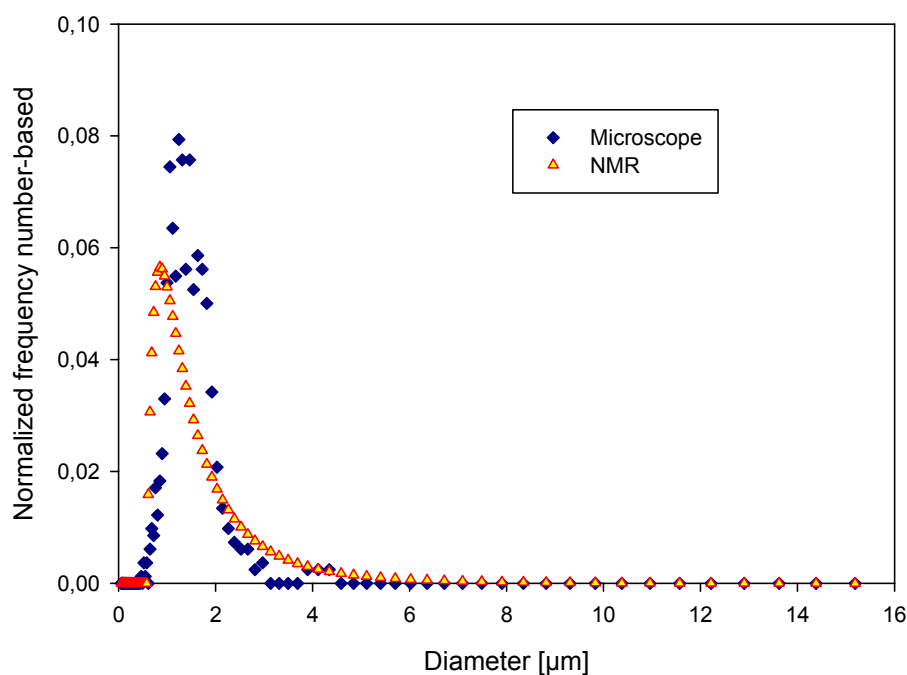


Figure 4.5 Comparison of the DSD of crude B from NMR and microscope; 10% water cut.

4.4 Reasons for discrepancies between the two techniques

As can be seen in table 4.1, the comparison of the two techniques are indeed promising. The correlation between the NMR and microscope was good the emulsions at water cuts 10 – 20 %. Both techniques used in this work have their limitations, and these limitations and how they can affect the data will be further discussed.

Considering the NMR, there are three potential effects that can influence the results. As indicated by table 4.1, the mean diameter from the NMR method increases more with the water cut than what is the case of the mean diameter from the microscope. The first explanation for the increased mean diameter from the NMR method is that of convection of the water droplets. If the droplets are moving during the diffusion measurements, the movement may affect the accuracy and influence the final droplet size distribution. Convection of water droplets will ultimately result in a distribution indicating larger droplets [34]. With increased water cut the overall viscosity of the emulsion changes, leading to a possible onset of convection of brine to the bottom of the sample tube. This movement largely exceeds the self diffusion which is used for probing the droplets size distribution. This may be wrongly interpreted as larger droplets as the apparent measured diffusion is biased towards

larger values due to convection. Another factor influencing the correlation between the two techniques is the stability of the emulsions formed. The stability of the emulsion is an important factor for the NMR measurements. Formation of a free water phase at the bottom of the NMR tube will perturb the final distribution since a free water phase will be perceived by the diffusion probing as large droplets. With a free water phase in the sample, the separate T_2 distribution of the water will not be representative of only the droplets in the emulsion phase, but will also include the bulk water. Figure 4.6 exhibits the NMR signal intensity as a function of the sample height of emulsions from crude B at different water cuts. The emulsions with water cuts from 10 to 30 % were all stable, as seen by the flat signal intensity, and a signal that increases with the water cut. Whereas for the emulsion of 40 % water cut sedimentation and coalescence of the droplets clearly occurs. The increase in signal intensity in the middle and lower part of the tube for the 40 % emulsion can be interpreted as an accumulation of droplets, and the large peak at the bottom of the NMR tube is indicative of the formation of a free water phase. The intensity profiles of figure 4.6 were also confirmed by visually examining the sample tube containing the emulsion after the measurements were completed. The emulsion of water cut 40% for crude B had formed a separate water phase.

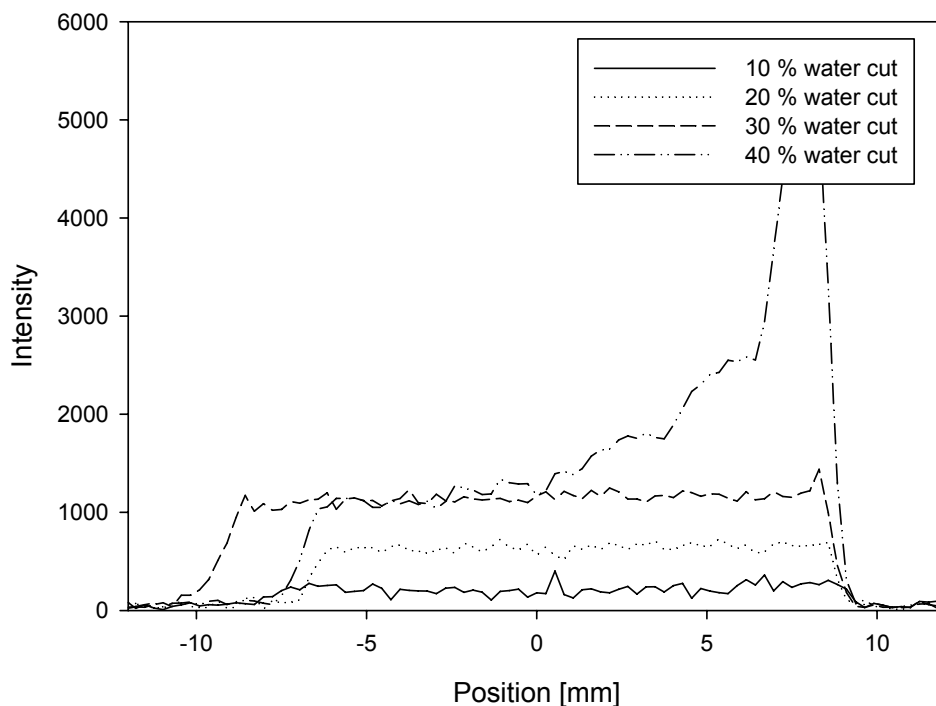


Figure 4.6 NMR signal intensity profile of crude B emulsions as a function of position. Bottom of sample is at ~10 mm, and top of sample is at ~ -10 mm.

There is ongoing work to develop a NMR-method capable of monitoring and measuring the size distribution of unstable emulsions. The position dependent signal intensity illustrated in figure 4.6 is a promising feature to study emulsion stability.

The third possible effect for decreasing correlation is due to the model used for NMR data interpretation. Depending on droplet size, the echo attenuation of the diffusion measurements can be modeled differently. The model used herein is based on diffusing molecules for which the mean squared displacement for unrestricted movement is much larger than the actual droplet sizes (section 2.1.3). With an observation time of a few milliseconds this model applies for droplets with diameter around $\sim 1 \mu\text{m}$. This is not the case for all the droplets within the emulsions with a higher water cut, as demonstrated by table 4.1. The validity of the simplification leading to equation 2.11 may not be valid for the larger droplets. However, as will be shown below, the correlation of the distributions from the microscope and the NMR is good for emulsions from crude C at various water cuts. Hence, the importance of this effect seems to be of minor importance compared to the other two effects as mentioned above.

4.5 Bimodal droplet size distribution

The emulsions prepared from crude C exhibited a bimodal distribution from the NMR data, as seen in figure 4.8. The bimodal shape of the distribution exemplifies the usefulness of the NMR method. In figure 4.8, the volume-based normalized frequency of the droplet sizes for 10 and 40 % water cut emulsions have been plotted. And the figure indicates a bimodal distribution, with modes around $1,8 \mu\text{m}$ and $4,5 \mu\text{m}$ in diameter for the emulsion of 10 % water cut. As the water cut increases, an increase in the modes and a shift of the share of the respective modes can be observed.

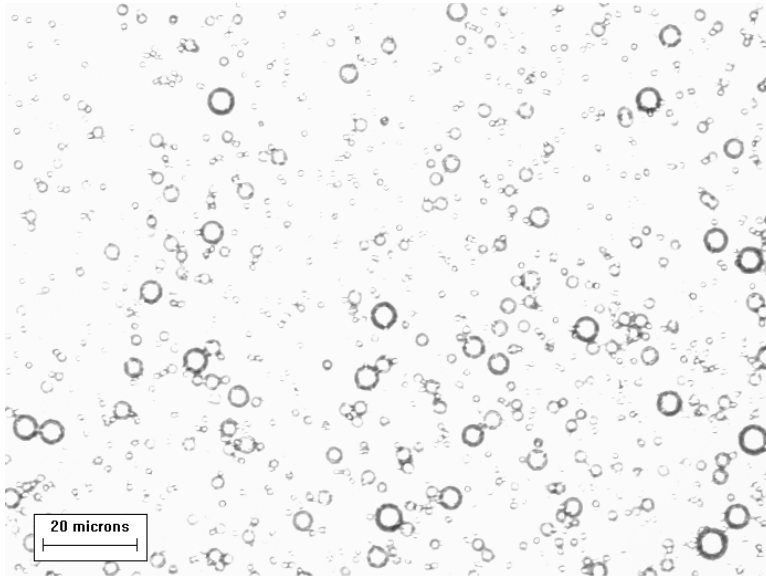


Figure 4.7 Microscope image of an emulsion of crude C, 40% water cut.

The increase in the share of larger droplet with increasing water cut is expected; increased water cut increases the probability of formation of larger droplets. The bimodal nature of the distributions of these emulsions was confirmed by the distribution obtained from the image analysis plotted in figure 4.9. The modes of the distributions from the image analysis are reasonably similar to the NMR results; around 1.3 μm and 4 μm in diameter, depending on the water cut. The bimodality is not that distinct for the emulsion with water cut 10 % in the microscope. However, at 40 % two peaks are clearly visible. The difference in modes and the amount of the different droplet sizes for the NMR and microscope data can be explained by the different weighting of the plots. The data plotted from the NMR is volume-based, whereas the data from the microscope is number-based. And as previously mentioned these two bases are not directly comparable. A volume-based distribution will underestimate the amount of the smallest droplets and vice-versa.

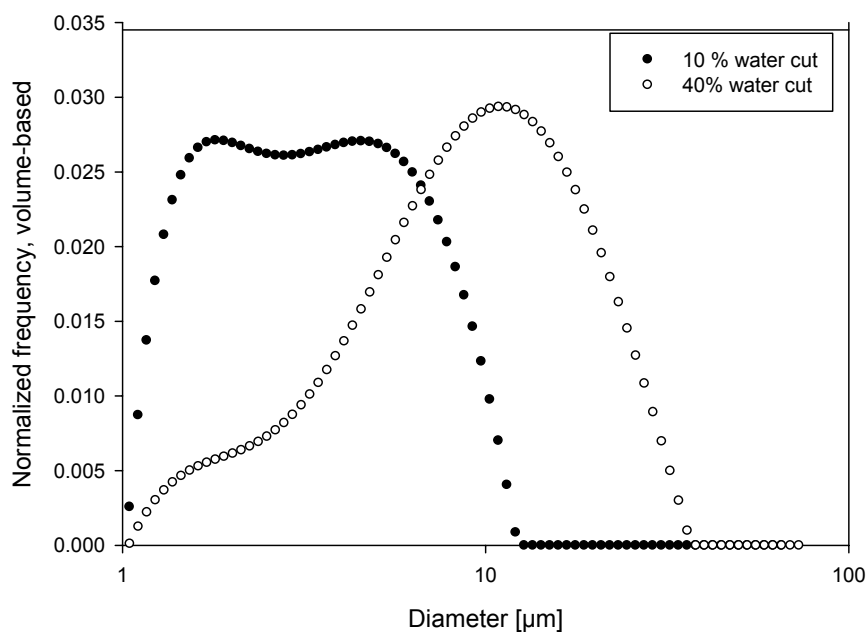


Figure 4.8 Emulsion droplet size distributions of crude C at different water cuts obtained by the NMR.

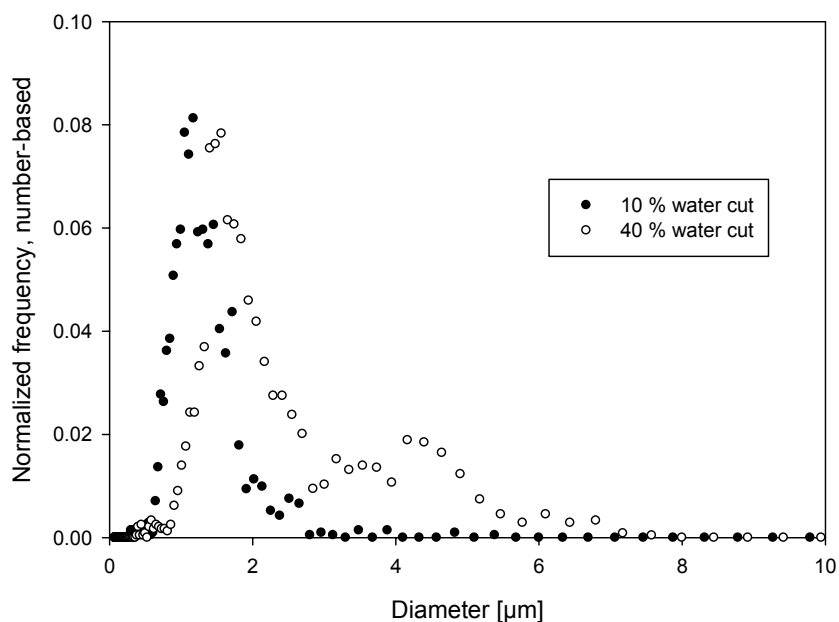


Figure 4.9 Emulsion droplet size distributions of crude C at different water cuts obtained by the microscope.

4.6 On the approximations in the pore size (S/V) distribution model

To be able to transfer the NMR measurements one must make an important approximation that relates to the duration of the gradient pulses. The literature makes use of three length scales, the diffusion length, the dephasing length and the pore length [37]. In the short time expansion developed by Mitra et al. [20] it was assumed piecewise smooth surfaces that only a small fraction of the probing molecules experienced, i.e. the diffusion length is much less than the pore length. Thus one could apply the square root of time attenuation of the diffusion coefficient to get the surface to volume ratio. As the droplets are getting smaller, the dephasing length may become comparable to the pore/droplet length. As long as there is a small deviation one should apply the corrected effective diffusion times as developed by Fordham et al. [38]. This correction will lead to larger average droplet sizes as the restricted diffusion during the gradient pulses is corrected for. However, in systems mainly consisting of small droplets, where the diffusion length becomes much larger than the droplet size, the Mitra model fails anyway due to a deviation from the square root of time dependency on the measured diffusivity. If it is apparent that the measured diffusion coefficient is attenuated significantly at the shortest observation time possible (~ 1 ms), the S/V ratio then cannot be found accurately. To measure the S/V for such a system by NMR the asymptotic level of the diffusion coefficient must be used. Then one may choose the experimental parameters such that $(6 D_0 t)^{1/2} \gg R_{\text{cavity}}$. Still there is a lower limit to what droplet sizes one may measure using this method. As the droplet sizes gets smaller the validity of the Gaussian approximation of the phases of the nuclear spins fails due to restricted diffusion during the gradient pulses, i.e the dephasing length becomes comparable and even larger than the typical droplet size. One may compensate for this effect by measuring the attenuation at different gradient pulse lengths and get a measure for the droplet size as a function of gradient pulse length. Then a fit of this functionality including an extrapolation back to zero gradient pulse length yields a gradient pulse length independent average droplet size.

Conclusion

This work has evaluated a LF-NMR method for the applications of obtaining droplet size distributions of petroleum crude oil emulsions with different water cut. An optical microscope was used as a reference technique. The correlation between the two techniques was overall good.

Compared to many other techniques, the NMR can analyze concentrated and opaque samples, such as petroleum emulsions. Measurements are performed within one minute, and no sample preparation is needed. One of the major advantages with the presented technique is its ability to obtain the droplet size distribution without making any assumptions on the shape of the distribution. This means that the method is capable of obtaining bimodal size distributions. Another potentially promising feature is the NMR signal profile which can be used to study emulsion stability.

Acknowledgments

The authors thank S bastien Simon for proof-reading the paper. Nils van der Tuuk Opedal thanks StatoilHydro for a PhD grant.

References

1. Asano, Y. and K. Sotoyama, Food Chemistry, 1999. **66**: p. 327-331.
2. Otsubo, Y. and R.K. Prud'homme, Rheologica Acta, 1994. **33**: p. 303-306.
3. Basheva, E.S., et al., Langmuir, 1999. **15**: p. 6764-6769.
4. Chakraborty, M., C. Bhattacharya, and S. Datta, Colloids and Surfaces A: Physiochem. Eng. Aspects, 2003. **224**: p. 65-74.
5. Coupland, J.N. and D.J. McClements, Journal of Food Engineering, 2001. **50**: p. 117-120.
6. Hemmingsen, P.V., et al., *Droplet Size Distributions of Oil-in-Water Emulsions under High Pressures by Video Microscopy*. 2nd Edition ed. Emulsion and Emulsion Stability, ed. J. Sjöblom. Vol. 132. 2006, Boca Raton: Taylor & Francis.
7. Tanner, J.E. and E.O. Stejskal, The Journal of Chemical Physics, 1965: p. 288-292.
8. Tanner, J.E. and E.O. Stejskal, The Journal of Chemical Physics, 1968. **49**: p. 1768-1777.
9. Goudappel, G.-J.W., J.P.M.v. Duynhoven, and M.M.W. Mooren, Journal of Colloid and interface Science, 2001. **239**: p. 535-542.
10. Fourel, I., J.P. Guillemin, and D.L. Botlan, Journal of Colloid and interface Science, 1995. **169**: p. 119-124.
11. Duynhoven, J.P.M.v., et al., European Journal of Lipid Science and Technology 2007. **109**: p. 1095-1103.
12. Kiokias, S., A.A. Reszka, and A. Bot, International Dairy Journal, 2004. **14**: p. 287-295.
13. Aichele, C.P., et al., Journal of Colloid and interface Science, 2007. **315**: p. 607-619.
14. Packer, K.J. and C. Rees, Journal of Colloid and interface Science, 1972. **40**(2): p. 206-218.
15. Li, X., J.C. Cox, and R.W. Flumerfelt, The American Institute of Chemical Engineers Journal, 1992. **38**(10): p. 1671-1674.
16. Balinov, B., O. Söderman, and T. Wärnheim, Journal of the American oil Chemists' Society, 1994. **71**(5): p. 513-518.
17. Enden, J.C.v.d., et al., Journal of Colloid and interface Science, 1990. **140**(1): p. 105-113.
18. Callaghan, P.T., K.W. Jolley, and R.S. Humphrey, Journal of Colloid and interface Science, 1983. **93**(2): p. 521-529.
19. Peña, A.A. and G.J. Hirasaki, Advances in Colloid and Interface Science, 2003. **105**: p. 103-150.
20. Mitra, P.P., P.N. Sen, and L.M. Schwatz, Physical Review B, 1993. **47**(14): p. 8565-8574.
21. Sørland, G.H., et al., Diffusion Fundamentals, 2007. **5**: p. 4.1-4.15.
22. Kärger, J. and D.M. Ruthven, *Diffusion in Zeolites and other Microporous Solids*. 1992, New York: Wiley.
23. Hurlimann, M.D., et al., Journal of Magnetic Resonance, Series A, 1994. **111**(2): p. 169-178.
24. Uh, J. and A.T. Watson, Industrial & engineering chemistry research, 2004. **43**: p. 3026-3032.
25. Cohen, M.H. and K.S. Mendelson, Journal of Applied Physics, 1982. **53**: p. 1127.
26. Balinov, B. and O. Söderman, *Emulsion - the NMR Perspective*. Encyclopedic handbook of Emulsion Technology, ed. J. Sjöblom. 2001, New York: Marcel Dekker.

27. Sørland, G.H., *Method for measuring the content of fat/oil in multi component system. Patent number 6946837*. 2005: United States.
28. Gu, G., et al., *Colloids and Surfaces A: Physiochem. Eng. Aspects*, 2003. **215**: p. 141-153.
29. Meiboom, S. and D. Gill, *The Review of Scientific Instruments*, 1958. **29**(8): p. 688-691.
30. Denkova, P.S., et al., *Langmuir*, 2004. **20**: p. 11402-11413.
31. McClean, J.D. and P.K. Kilpatrick, *Journal of Colloid and interface Science*, 1997. **196**: p. 23-34.
32. Peña, A.A. and G.J. Hirasaki, *NMR Characterization of Emulsions. Emulsion and Emulsion Stability*, ed. J. Sjöblom. Vol. 132. 2006, Boca Raton: Taylor & Francis.
33. Dalen, G.v., *Journal of Microscopy*, 2002. **208**: p. 116-133.
34. Zhang, X., C.-G. Li, and M.-L. Liu, *Analytical Chemistry*, 2001. **73**: p. 3528-3534.